Purdue University
Purdue e-Pubs

International Refrigeration and Air Conditioning Conference

School of Mechanical Engineering

2006

Experimental Research and CFD Simulation on Microchannel Evaporator Header to Improve Heat Exchanger Efficiency

Zhihai Gordon Dong
American Power Conversion Corp.

John Bean
American Power Conversion Corp.

EXPERIMENTAL RESEARCH AND CFD SIMULATION ON MICROCHANNEL EVAPORATOR HEADER TO IMPROVE HEAT EXCHANGER EFFICIENCY

Zhihai Gordon Dong[1], John Bean Jr.[2]

[1]Research and Development, NetworkAir Dept.,
American Power Conversion Corp.
801 Corporate Center Dr., St. Charles, MO, US, 63304
Email: gordon.dong@apc.com

[2]Research and Development, NetworkAir Dept.,
American Power Conversion Corp.
801 Corporate Center Dr., St. Charles, MO, US, 63304
Email: john.bean@apc.com

ABSTRACT

Microchannel evaporator performs superior heat transfer efficiency and capacity at compact size comparing with conventional tube-fin evaporator. Design an appropriate coil header assembly is one of major tasks, which could affect the desired heat exchanger efficiency and capacity. An experimental investigation of three coil inlet header configurations, which are single, dual and distributor inlet headers, is conducted in the paper. A practical evaluation method, by means of measuring air temperature differential across coil to evaluate refrigerant distribution uniformity in coil header, is introduced. CFD models are also generated to simulate refrigerant liquid flow contours of these three inlet header configurations. Finalize the research, the distributor header configuration appears the most uniform distribution in conjunction with symmetrical flow distribution. The dual inlet header configuration also significantly improves distribution uniformness and symmetry comparing with the single inlet header configuration.

1. INTRODUCTION

1.1 Introduction of microchannel heat exchanger

A microchannel heat exchanger appears advanced characters comparing with a conventional round tube-fin heat exchanger. Refrigerant flows through multiple microchannel flat tubes, which contain microchannels ports rather than single wall round tubes. This significantly enhances the heat transfer area and overall film coefficient of the microchannel heat exchanger. High efficiency of the microchannel heat exchanger enables the heat exchanger to be made in smaller size, light weight, and yet has the same performance as a conventional round tube-fin heat exchanger. Refrigerant charge of the cooling system is also reduced.

Due to many advantages of microchannel heat exchanger, it has been widely applied in residential air conditioning and automotive industry.

However, comparing with a round tube-fin heat exchanger, microchannels ports causes higher refrigerant pressure drop across heat exchanger, it might be an issue to some systems. Condensation and defrost of microchannel coil are also major issues for refrigeration and air conditioning applications. The uniformity of refrigerant distribution within coil inlet header is another major issue for microchannel heat exchanger. A properly designed coil inlet header should uniformly distribute refrigerant into microchannels, and refrigerant would perform sufficient heat transfer inside microchannels tubes. Eventually, coil cooling efficiency is optimized and capacity is maximized. On the contrary, a defective coil header assembly could cause uneven refrigerant flow inside microchannels and reduce coil cooling efficiency and capacity. In the worst situation, the defective header design might cause the danger of gas and liquid flow separation, which could significantly damage coil heat transfer performance. Therefore, to achieve uniform refrigerant distribution, the coil header configuration and orientation becomes to be a very important design task.

1.2 A refrigerant liquid pumping cooling system for data center air conditioning application

The major duty of a data center air conditioning system is to remove sensible heat, which is generated by electronic equipments. Condensation is controlled and minimized in the system. Ideally, sensible heat ratio of this air conditioning system would equal to one. Modern servers are integrated into limit space. Heat load density in the space is high. A compact air conditioning system with high cooling efficiency and capacity needs to be developed to remove this high density heat flux.

A R134a liquid pumping cooling system is introduced to this application. The cycle of system circuit is shown in Figure (1).

In the diagram, subcooled liquid R134a enters pump intake at state point (1) to process adiabatic compression. Further subcooled liquid R134a leaves pump discharge port at state point (2). State point (2) to (3) presents liquid R134a flows through liquid line and reaches to inlet of evaporator. From state point (3) to (4), subcooled liquid is vaporized in evaporator. Slight superheated gas leaves evaporator at state point (4) and return back to condenser inlet at state point (5) via a suction line. R134a gas rejects heat to chilled water in condenser, and it becomes subcooled liquid. The subcooled liquid returns back to pump intake at state point (1) and cycle starts over again.

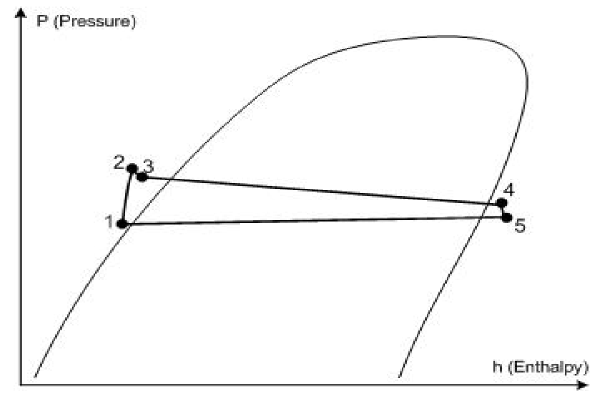

Figure (1) R134a liquid pumping cooling system cycle

1.3 Microchannel heat exchanger in the refrigerant liquid pumping cooling system

The microchannel coil is horizontally installed in space above two symmetrical heat loads. Upon means of control coil evaporating temperature, condensation is avoided to be generated on coil. However, due to subcooled liquid R134a flows into the large dimensional coil inlet header (approx 23" long), a proper coil inlet header configuration becomes important issue to accomplish refrigerant uniform distribution into microchannels.

1.4 Three configurations of microchannel coil inlet header

To optimize coil inlet header assembly, three configurations of microchannel coil inlet header are conducted and investigated in this paper. These three configurations - single, dual and distributor inlet headers are illustrated in Figure (2).

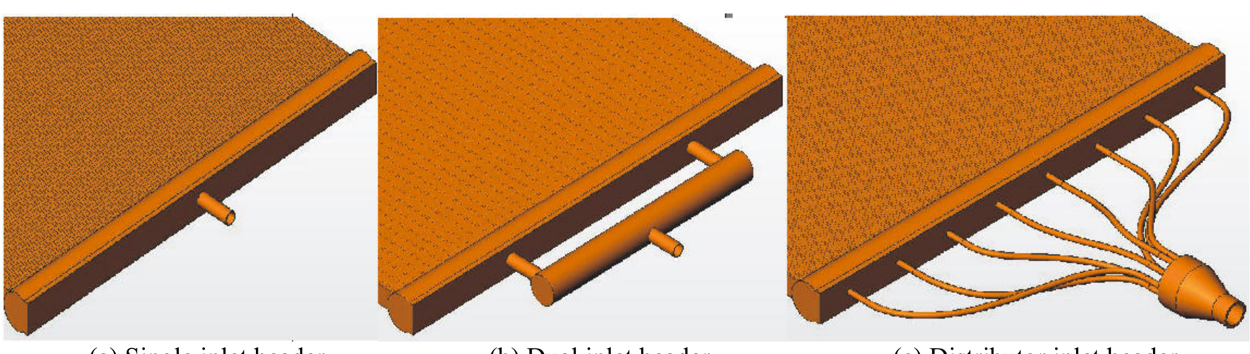

(a) Single inlet header (b) Dual inlet header (c) Distributor inlet header

Figure (2) Three configurations of microchannel coil inlet header

The single inlet header is constructed by a single round tube, which is simply welded to center of coil inlet manifold in perpendicular direction. The dual inlet header employs a secondary header, which is jointed to the coil inlet manifold via two round tubes at ¼ and ¾ length of coil inlet manifold. Main liquid entry line is connected to center of the secondary header. The entire dual inlet header assembly is furnace welded. Refrigerant liquid flows into the secondary header first. It is subsequently divided into two braches by the two round interjunction tubes, and flows into coil inlet manifold. The third configuration is the distributor inlet header. Refrigerant liquid flow is evenly divided inside hollow conical portion of the distributor. A group of small capillary tubes are connected to the distributor to pick up the branched refrigerant flow. They deliver refrigerant liquid into coil inlet manifold at even portions.

2. THE APPROACH TO EVALUATE REFRIGERANT DISTRIBUTION UNIFORMITY INSIDE COIL INLET HEADER

2.1 Heat transfer and thermodynamic process inside microchannel tube

To simplify heat transfer and thermodynamic analysis inside microchannel ports, we consider the group of microchannel ports as one single microchannel tube. The process is illustrated in Figure (3).

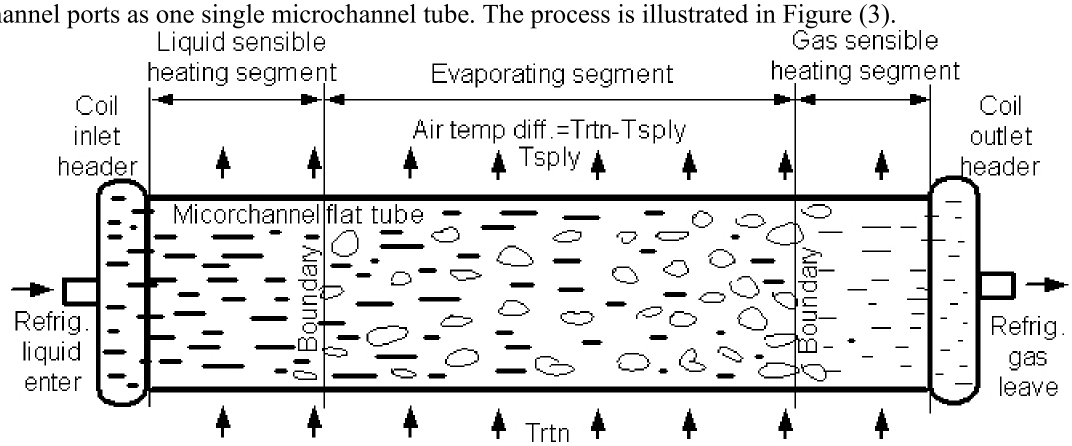

Figure (3) Refrigerant heat transfer and thermodynamic process inside microchannel tube (Not to scale)

As shown in Figure (3), refrigerant flow inside microchannel tube is composed by three segments, which are liquid sensible heating, evaporating, and gas sensible heating segments. The local convective heat transfer flow rate Q_{hx} is calculated in Equation (1).

$$Q_{hx} = \int_0^A h \, \Delta t_{hx} \, dA \qquad (1)$$

The convective heat transfer coefficient h is strong dependent upon the refrigerant's physical properties, situation and Reynolds number. It is much higher within evaporating (two-phase flow) segment due to bubble generation and other major factors. Heat transfer flux appears extremely active within this area, while the heat transfer density is much lower within subcooled and superheated segments (one-phase flow).

There is no phase change within liquid sensible heating and gas sensible heating segments. Refrigerant sensible heat flow rate in these areas is donated in Equation (2).

$$Q_r = m_r \, C_{pr} \, \Delta t_r \qquad (2)$$

Refrigerant performs phase change in evaporating area, the latent heat flow rate of refrigerant in the area is shown in Equation (3).

$$Q_r = m_r \, \lambda_r \qquad (3)$$

R134a latent heat λ_r is almost 20 times larger than its isobaric specific heat C_{pr} within this heat exchanger working range. Heat transfer flux in microchannel is primarily contributed by refrigerant's latent heat.

Airflow vertically flows through microchannel tube, and it rejects sensible heat to refrigerant. The airflow temperature differential across microchannel tube Δt_a is expressed in Equation (4).

$$\Delta t_a = t_{rtn} - t_{sply} = Q_a / (m_a \, C_{pa}) \qquad (4)$$

Air isobaric specific heat C_{pa} approximately equals to 1.01(kJ/kg- K). When air mass flow rate m_a is uniformly remained as constant, airflow temperature differential crossing coil Δt_a is direct proportional as function of air sensible heat flow rate Q_a.

2.2 The approach to evaluate distribution uniformity of refrigerant flow inside coil inlet header

Viscous fluid convective heat exchange is difficult to analyze and predict. In practice, many of this type of heat transfer analysis are treated empirically. It is difficult to inspect refrigerant flow rate distribution inside coil inlet header directly. Instead of direct pursue flow distribution contour inside coil header, a thermodynamic and heat transfer analysis in microchannel portion could be a strong indicator of refrigerant distribution status inside coil inlet header. It is a practical way to evaluate the coil inlet header distribution uniformity.

As been described before, within the subcooled liquid and superheated gas segments, heat transfer coefficient h and heat transfer flow rate Q_{hx} remain at relative lower level. Airflow temperature difference across these microchannel segments Δt_a appears relative small. Within evaporating segment, although the heat transfer coefficient h is various, Δt_a is relative much higher as result of strong heat transfer flux. Airflow temperature differential Δt_a across microchannel appears significantly larger. Therefore, airflow temperature differential across microchannel Δt_a directly indicates refrigerant status inside microchannel tube. When Δt_a is significant higher, refrigerant is in two-phase status, and it performs strong heat transfer inside microchannel tube. When Δt_a is lower, it indicates that refrigerant is either in liquid or gas state inside microchannel tube.

Refrigerant mass flow rate is various between microchannel tubes due to refrigerant's uneven distribution inside coil header. The larger mass flow inside microchannel is, the further behind transient locations of segment will be. The gradient of segment boundary (transient) locations forms two curves of parabola (refer to Figure (9)) on microchannel coil surface. These two parabolas divide coil into three segments of liquid sensible heating, evaporating and gas sensible heating. A degenerate parabola indicates a better uniformness of refrigerant flow distribution inside coil inlet header. On the contrary, an evolvable parabola donates the worse refrigerant flow distribution inside coil inlet header.

3. EXPERIMENTAL AND DATA ACQUISITION SYSTEM

3.1 The R134a experimental cooling system and components

The experimental system schematic is shown in Figure (4). Refrigerant liquid pump (A) is controlled by a variable speed controller (B). A motorized three-way valve is used to modulate building chiller water flow, which flows through a brazed plate condenser (E). The combination of motorized three-way valve and variable speed liquid pump maintain the desired evaporating temperature and superheat (state point (4)). Axial fan array (D) delivers airflow through the evaporator (C) at a desired constant airflow rate. A test chamber is conducted to simulate the natural work environment. Three microchannel coils (C), which are assembled with three configurations of inlet header, is horizontally installed in space above symmetrical heat loads. Figure (5) shows the installation.

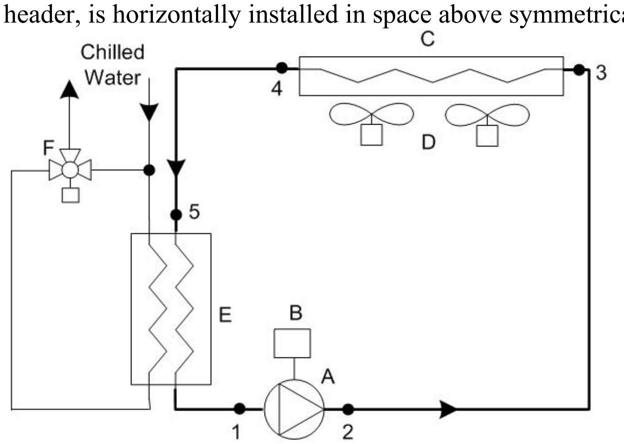

Figure (4) Schematic of experimental R134a liquid pumping system

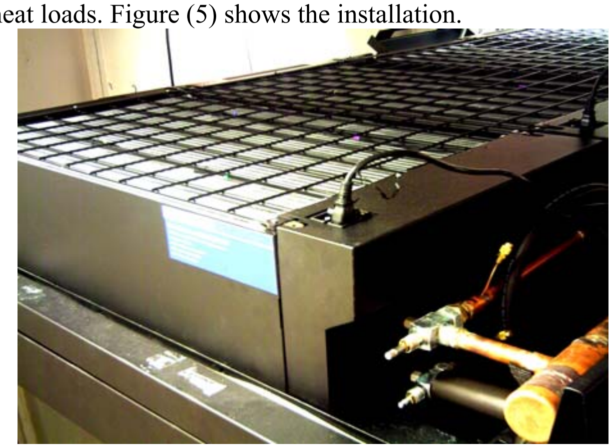

Figure (5) Microchannel coil assembly is horizontally installed in space above symmetrical heat loads

3.2 Data acquisition instrumentation

An Agilent 34970 data logger is used in the data acquisition system. Capacitance type pressure transducers are installed at evaporator inlet and outlet to measure R134a entering and leaving pressure. Thermistors are mounted to the same location to measure R134a entering and leaving coil temperature. The evaporator inlet subcooling and outlet superheating temperatures are computed by combination of these pressure and temperature readings. Ideally, Δt_a across each microchannel tube should be measured to locate these segment transient locations, which was previously introduced in this paper. However, this will require an extremely large number of temperature measure nodes on coil both sides. To simplify measurements, the coil surface is divided into nine of even zones on coil each side. As shown in Figure (6), an array of 3 x 3 temperature measure nodes (located at center of each zone) on coil each side is arranged in this experiment. Thermistors are installed at these discrete points to measure return air temperature (T_{rtn} at bottom surface of coil) and supply air temperature (T_{sply} at top surface of coil).

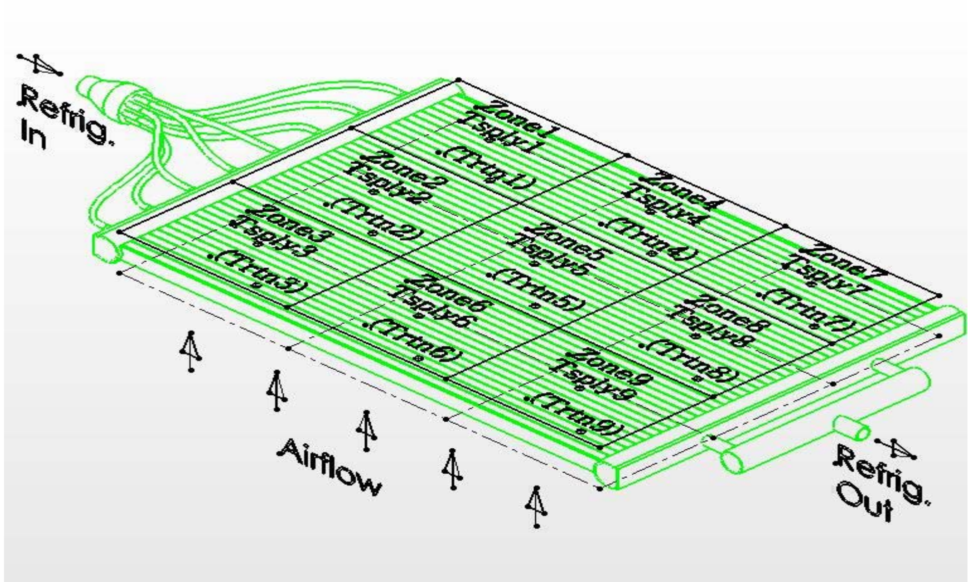

Figure (6) Coil zones (nine on coil each side) and temperature measure nodes layout

4. EXPERIMENT RESULT AND DISCUSSION

4.1 Test result and airflow temperature differential across coil

Air mass flow rate is maintained at a constant during tests. R134a evaporating temperature is maintained at 63F, and superheat at coil outlet is controlled at 3.9°C (7°F). Subcooling at coil inlet stays at 4.4°C (8°F). Average readings of supply air temperatures T_{sply} and return air temperatures T_{rtn} (in parentheses) at discrete center points of these zones are listed in Figure (7). Coils are presented as 2D top views in this Figure.

Refrig. flow direction → (Inlet Header on left, Outlet Header on right)

Inlet Header				Outlet Header
	Zone1 23.04C (31.76C)	Zone4 21.29C (31.64C)	Zone7 24.93C (30.75C)	
	Zone2 25.67C (30.89C)	Zone5 21.70C (32.01C)	Zone8 21.73C (30.63C)	
	Zone3 25.0C (30.95C)	Zone6 20.95C (31.52C)	Zone9 24.28C (31.38C)	

(a) Single Inlet Header Coil

Inlet Header				Outlet Header
	Zone1 21.97C (30.59C)	Zone4 21.87C (31.5C)	Zone7 21.53C (30.68C)	
	Zone2 23.69C (31.2C)	Zone5 21.37C (31.06C)	Zone8 21.96C (31.54C)	
	Zone3 22.69C (31.44C)	Zone6 22.52C (32.46C)	Zone9 23.69C (32.24C)	

(b) Dual Inlet Header Coil

Inlet Header				Outlet Header
	Zone1 22.34C (31.16C)	Zone4 20.94C (30.64C)	Zone7 23.44C (32.38C)	
	Zone2 23.36C (31.84C)	Zone5 21.67C (31.31C)	Zone8 21.41C (31.06C)	
	Zone3 22.16C (30.73C)	Zone6 21.25C (31.02C)	Zone9 22.67C (32.01C)	

(c) Distributor Inlet Header Coil

Figure (7) T_{sply} and T_{rtn} (in parentheses) measurements at coil each zone

Refrig. flow direction → (Inlet Header on left, Outlet Header on right)

Inlet Header				Outlet Header
	Zone1 8.72C	Zone4 10.35C	Zone7 5.82C	
	Zone2 5.22C	Zone5 10.31C	Zone8 8.89C	
	Zone3 5.95C	Zone6 10.57C	Zone9 7.10C	

(a) Single Inlet Header Coil

Inlet Header				Outlet Header
	Zone1 8.62C	Zone4 9.63C	Zone7 9.14C	
	Zone2 7.51C	Zone5 9.68C	Zone8 9.49C	
	Zone3 8.74C	Zone6 9.94C	Zone9 8.54C	

(b) Dual Inlet Header Coil

Inlet Header				Outlet Header
	Zone1 8.82C	Zone4 9.69C	Zone7 8.93C	
	Zone2 8.48C	Zone5 9.63C	Zone8 9.65C	
	Zone3 8.57C	Zone6 9.77C	Zone9 9.34C	

(c) Distributor Inlet Header Coil

Figure (8) Air temperature differential Δt_a across coil each zone

As defined in Equation (4), airflow temperature differential across microchannel is calculated at $\Delta t_a = t_{rtn} - t_{sply}$. Figure (8) donates the Δt_a across each coil zone.

4.2 Analysis of refrigerant distribution uniformity inside coil inlet header

In general, middle portion (zone4, zone5 and zone6) of coil should be mainly occupied by refrigerant evaporation. Here we choose zone6 as the benchmark zone, and assume this zone is fully fulfilled with refrigerant two-phase mixture. Airflow temperature differential across each coil zones could be illustrated as percentage ratio to Δt_a of zone6. Each percentage ratio donates weight of refrigerant evaporation portion within that zone. By means of converting the percentage ratio into linear scale, appropriate trendlines across these points can be drawn. These curves are in shape of parabola as shown in Figure (9). Although each parabola is not physical segment transient location (boundary), it is excellent substitute (trendline) to represent the segment transient's location and tendency. Each coil is divided into three segments by two parabolas. These three areas are approx. liquid sensible heating, evaporating, and gas sensible heating segments of that coil.

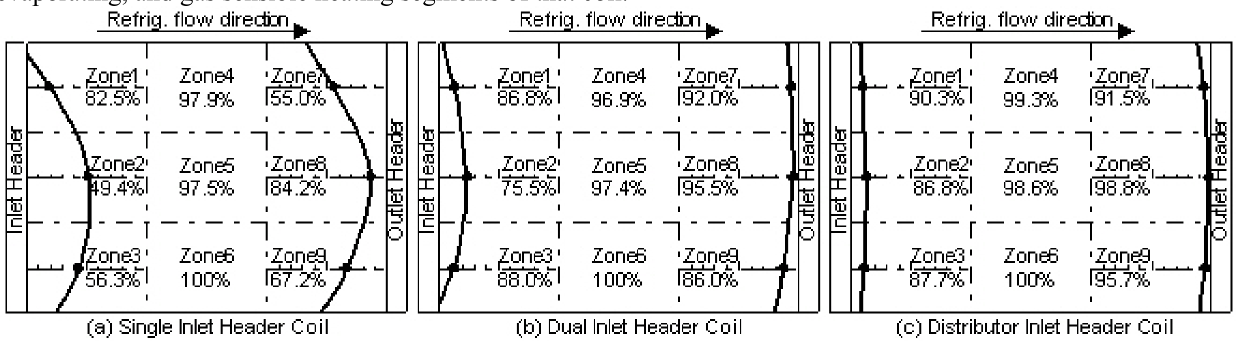

Figure (9) Weight ratio of evaporation within each zone and coil segment trendlines on coil surface

Analyze these trendlines in Figure (9), the most evolvable parabola along the axial direction appears on single inlet header coil. It indicates the single inlet header coil performs the worst refrigerant flow distribution among these three coils. On the contrary, the distributor inlet coil header appears the most uniform refrigerant flow distribution. The dual inlet coil header significantly improves refrigerant flow distribution comparing with the single inlet coil header.

Another phenomenon is the inclination on parabola symmetry. The inclination of turbulent flow has been minimized prior to enter into coil inlet header. Therefore, the inclination inside coil header is mainly caused by asymmetrical geometric factors of inlet header and surrounding area. The parabola for the single inlet header coil appears the most asymmetrical among the three types of coil. This is because that refrigerant liquid flows into the single inlet header via single tube, any asymmetric factor of the inlet tube and surround flow path could cause an obvious inclination on liquid flow direction. Furthermore, it influences the symmetry of distribution. In the case of dual inlet header, refrigerant liquid is divided into two branches to flow into the coil header manifold. This reduces the influence by asymmetric factors of each single branch.

4.3 Experiment result accuracy

The experiment was conducted inside a test chamber to simulate the real working environment. Return air temperature was not perfect uniformed at these discrete points on the coil air return surface. This affected air temperature differential Δt_a crossing coil at certain level. However, accomplishing with coil header improvement, the gradient of Δt_a is uniformed significantly. This donates that a certain level of return air temperature gradient did not affect the experiment conclusion.

5. NUMERICAL STUDY OF THREE INLET HEADER CONFIGURATIONS

5.1 CFD model characterization and assumption

A "CFDesign" software is utilized to algorithmically compute the refrigerant liquid flow contours inside these three types of inlet header.

Refrigerant flow is assumed as a single-phase, incompressible viscous turbulent flow at steady state, and process is adiabatic. The CFD model geometry of the header and coil assembly is characterized as a 3D smooth internal pipe flow. Boundary condition is constrained at 1 gpm of volume flow rate at coil inlet and 0 Pa pressure at coil exit. Coil material is given as aluminum, and fluid type is R134a. The element mesh size is set at 0.5", with total element number of approx. 10k. Total number of compute iterations is set at (100).

5.2 Compute result and velocity magnitude contours

The CFD computed velocity magnitude contours of refrigerant flow inside coil inlet header is showed in Figure (10). Obviously, the single inlet header concentratedly distributes refrigerant into middle portion of microchannel coil; the dual inlet header significantly improves the refrigerant distribution uniformity inside inlet coil header; and the distributor inlet header performs the most uniformed refrigerant distribution.

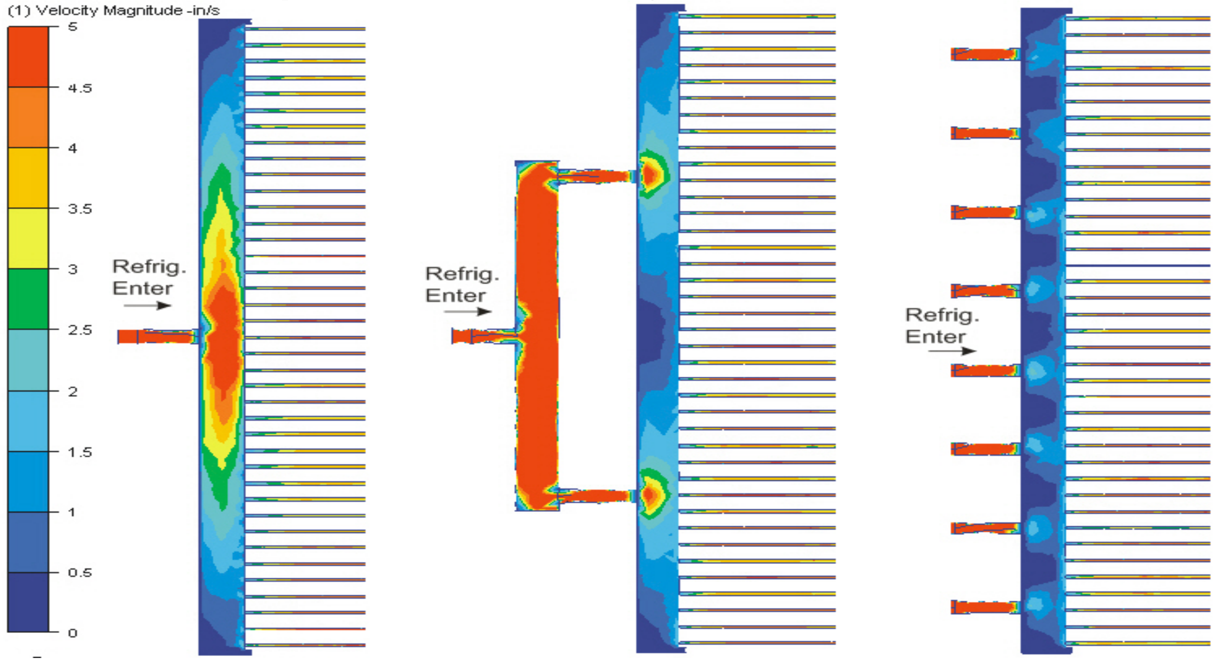

(a) Single inlet header (b) Dual inlet header (c) Distributor inlet header

Figures (10) Refrigerant velocity magnitude contours inside inlet coil header

5.3 CFD analysis of inclination on refrigerant distribution symmetry by inlet header tube slope

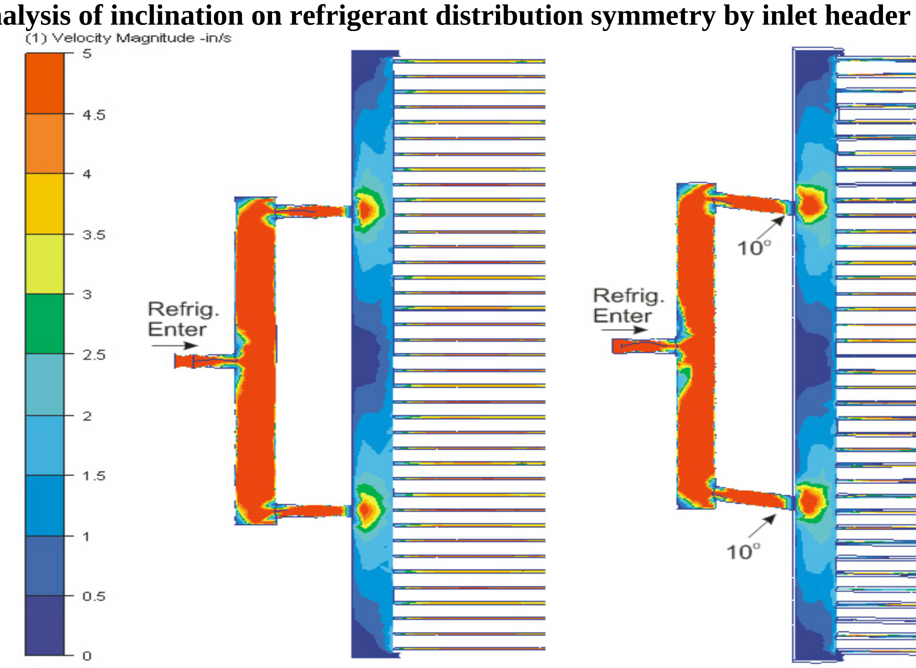

(a) Dual inlet header with no tube slope (b) Dual inlet header with 10^{o} tube slope

Figure (11): Symmetry inclination of refrigerant velocity magnitude contours by inlet header tube slope

As previous stated in the paper, inclination of turbulent flow and many asymmetric geometric factors of inlet header and surrounding flow path could cause symmetry inclination on header liquid distribution. The slope of inlet header tube is one of these geometric factors. To demo the inclination, a 10-degree inlet tube slope angle is added to the dual inlet coil header model. The compute result is illustrated in Figure (11). As showed in the Figure, refrigerant velocity magnitude axis center is moved downwards due to the 10^o of inlet tube slope.

7. CONCLUSIONS

An appropriate coil inlet header assembly design is one of the essential tasks to improve the microchannel heat exchanger heat transfer efficiency and maximize the cooling capacity.
Among these three inlet header configurations, the distributor header performs the most uniform refrigerant liquid flow distribution conjunction with good flow symmetric contour. The dual inlet configuration significantly improves refrigerant flow distribution uniformity and symmetry.

NOMENCLATURE

Symbol	Description	Unit	Subscripts	
A	Heat transfer area	(m^2)	a	Air
C	Specific heat capacity	(J/kg- ^oC)	hx	Heat exchanger
h	Convective heat transfer coefficient	(W/m^2- ^oC)	p	Isobaric
m	Mass flow rate	(kg/s)	r	Refrigerant
t	Temperature	(^oC)	rtn	Air return
Q	Heat flow rate	(W)	sply	Air supply
Δ	Differential			
λ	Latent heat of vaporization	(J/kg)		

REFERENCES

Bergles, A.E., Lienhard V, J. H., Kendall, G.E., Griffith, P., 2003, Boiling and Evaporation in Small Diameter Channels, *Heat Transfer Eng*., vol. 24, no. 1, p. 18 -40.

Kakac, S., Liu, H., 2002, *Heat Exchangers Selection, Rating and Thermal Design,V2.*, CRC Press, US, 501 p.

Kim, J., Groll, 2003, Performance and Reliability of Microchannel Heat Exchangers in Unitary Equipment, *The Ray W. Herrick Lab., Purdue Univ.,* 10 p.

Zhao, Y., 2001, Previous Studies on Microchannel Heat Transfer, Chapter 2.2, *In*: Ohadi, M.M., Radermacher, R., *Microchannel Heat Exchangers with Carbon Dioxide*, Maryland Univ., p. 11-17

ACKNOWLEDGEMENT